

Distribution of Magnetization in Microwire Magnetoimpedance Elements

A. T. Morchenko, L. V. Panina, and V. G. Kostishyn

Department of Electronics Materials Technology, National University of Science and Technology (MISiS),
Moscow, 119049 Russia
e-mail: dratm@mail.ru

Abstract—An important prerequisite for successfully developing highly sensitive magnetic field sensors based on amorphous ferromagnetic microwires is to study the conditions of excitation and the effect external magnetic fields on magnetoimpedance in amorphous ferromagnetic microwires. The distribution of magnetization is considered a function of the magnetic properties of a wire material, the bias current, and the strength and orientation of the external magnetic field.

DOI: 10.3103/S1062873814110215

INTRODUCTION

A problem of great interest in today's microsystem technology is developing sensors of weak magnetic fields and currents [1]. The magnetoimpedance (MI) effect allows us to create sensors with abilities exceeding those of devices built on the basis of the familiar magnetoresistive effect [2, 3]. The MI effect is observed most strongly in cylindrical amorphous wires where a specific structure of magnetic anisotropy with mainly circular or spiral (helical) distributions of saturation magnetization in the external layer of a conductor with longitudinal orientation in the core is formed to obtain high values of the output signal. It is assumed that the magnetodynamics of such systems when using alternating current is due to small rotations of magnetization vector \vec{M} with respect to its steady-state position. External magnetic field \vec{H} applied along the axis of the conductor changes the orientation of the magnetization in the external layer of the microwire, along with its effective magnetic permeability μ_{eff} and inductance. The relations associating the magnitude of the recorded signal with the external conditions and characteristics of the conductor's material [4, 5] contain the values of effective magnetic permeability and skin-layer thickness:

$$V_c = R_0(\pi n a) \frac{a}{2\delta_0} [(\sqrt{\mu_{\text{eff}}} - 1) \sin 2\psi] i. \quad (1)$$

where n is the number of turns per unit length of the detecting coil; ψ is the angle between vector \vec{M} and the axis of the wire; i is the amplitude of the excitation current; and δ_0 is the skin-layer thickness at $\mu_{\text{eff}} = 1$, determined with the expression

$$\delta_0 = c[\rho/(2\pi\omega)]^{1/2}, \quad (2)$$

where c is the speed of light, ω is the circular frequency of the alternating current, and ρ is the specific electric resistance of the material of the ferromagnetic conductor.

Surface impedance thus depends on the dynamic magnetic permeability and orientation of the steady-state component of magnetization, which in particular can be highly sensitive to external conditions.

DISTRIBUTION OF MAGNETIZATION IN THE SKIN LAYER OF MI WIRE UNDER THE IMPACT OF MAGNETIC FIELD

In [6], we solved the problem of the distribution of magnetization under the effect of an external field applied along the axis of a microwire; in [7, 8], the effect the orientation of an external magnetic field on the signal of a sensor element was studied experimentally. In this work, the problem of the distribution of magnetization as a function of the material parameters of a conductor, the excitation mode (bias current), and external conditions (strength and orientation of external magnetic field) is considered in the most general form.

A scheme of the distribution of magnetization in a skin layer is shown in Fig. 1 for helical anisotropy and an arbitrary direction of the external field.

In the considered geometry, the z -axis of the conductor is the polar axis of the spherical and cylindrical coordinate systems. The direction of easy magnetization in the skin layer is shown by spiral lines. Point O on the cylindrical surface of the wire in which the current magnetization state is considered is the origin of the coordinate system $x'y'z'$. Its position in the xy -plane is given by parameter φ , the azimuthal angle of

the polar coordinate system. The equilibrium orientation of magnetization vector \vec{M} is described by the polar ψ and azimuthal ϕ angles in the system $x'y'z'$, which are determined by the material parameters of the conductor, the current, and the external magnetic field. Angle θ shows the deviation of vector \vec{H} from the z -axis of the conductor in the direction of the y -axis. The direction of the easy magnetization axis at point O is determined by tangent \vec{K} to the screw line of light magnetization, the helix pitch is given by angle ψ_K between the tangent and the $x'Oy'$ plane, and the projection of the tangent onto this plane forms angle φ with the y' -axis.

The existence of domains complicates the pattern of magnetization distribution, so they are usually suppressed using bias magnetic field \vec{H}_b created by the constant component of the excitation current and magnetizing the wire in the circular direction. For a cable diameter of $2a$, the circular field strength on the surface can be estimated from the formula of calculating $H_b = i/a$ (the field is in G, the radius of the wire in μm , the current in mA).

If the external field is parallel to the axis of the wire ($\theta = 0$), the tangential component of vector \vec{M} neither creates demagnetizing fields nor contribute to magnetostatic energy E_M (the energy of shape anisotropy). The radial component of magnetization can emerge when $\theta \neq 0$, leading to an increase in the magnetostatic energy. The total energy of the system with allowance for Zeeman energy E_H and energy of anisotropy E_K is

$$E = E_H + E_K + E_M. \quad (3)$$

where $E_H = -\vec{M}\vec{H}_t$, $\vec{H}_t = \vec{H} + \vec{H}_b$; $E_K = K\sin^2(\widehat{\vec{M}\vec{K}}) = K[1 - \cos^2(\widehat{\vec{M}\vec{K}})]$; and $E_M = \sum N_j M_j^2 / 2$. K is the anisotropy constant; N_j denotes demagnetizing coefficients with respect to the j th axis of the coordinates; and the components of the magnetic field and magnetization vectors can be written using the param-

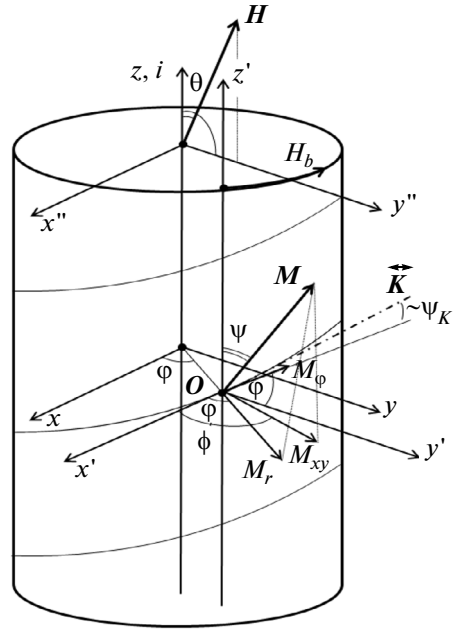


Fig. 1. Geometry and main characteristics of a model sensor element.

eters of Cartesian, spherical, and cylindrical coordinates:

$$H_{tx} = -H_b \sin \varphi, \quad H_{ty} = H_b \cos \varphi + H \sin \theta, \quad (4)$$

$$H_{tz} = H \cos \theta,$$

$$M_x = M \sin \psi \cos \phi, \quad M_y = M \sin \psi \sin \phi, \quad (5)$$

$$M_z = M \cos \psi,$$

$$M_\phi = M \sin \psi \sin(\phi - \varphi), \quad (6)$$

$$M_r = M_{xy} \cos(\phi - \varphi) = M \sin \psi \cos(\phi - \varphi).$$

In this case, $N_\phi = N_z = 0$. For a thin, uniformly magnetized cylindrical thread, $N_r = N_x = N_y = 2\pi$; however, because the magnetoimpedance is determined by the thin surface layer as a result of the skin effect, we must assume that $N_r \approx 4\pi$ in the direction of its normal, just as with the plane.

In the most general case of the problem's formulation, we thus have

$$E_H = -M[-H_b \sin \varphi \sin \psi \cos \phi + (H_b \cos \varphi + H \sin \theta) \sin \psi \sin \phi + H \cos \theta \cos \psi] \quad (7)$$

$$= -M[H_b \sin \psi \sin(\phi - \varphi) + H \sin \theta \sin \psi \sin \phi + H \cos \theta \cos \psi],$$

$$E_K = K\{1 - [\sin \psi \sin(\phi - \varphi) \cos \psi_K + \cos \psi \sin \psi_K]^2\}, \quad (8)$$

$$E_M = \frac{N_r M_r^2}{2} = 2\pi M^2 \sin^2 \psi \cos^2(\phi - \varphi). \quad (9)$$

Solving the system of equations obtained from the conditions of the total energy's extremum in the general form,

$$\begin{aligned} \frac{\partial E}{\partial \psi} = & -M[H_b \cos \psi \sin(\phi - \varphi) + H \sin \theta \cos \psi \sin \phi - H \cos \theta \sin \psi] \\ & - 2K[\sin \psi \sin(\phi - \varphi) \cos \psi_K + \cos \psi \sin \psi_K][\cos \psi \sin(\phi - \varphi) \cos \psi_K - \sin \psi \sin \psi_K] \\ & + 4\pi M^2 \sin \psi \cos \psi \cos^2(\phi - \varphi) = 0, \end{aligned} \tag{10}$$

$$\begin{aligned} \frac{\partial E}{\partial \phi} = & -M[H_b \sin \psi \cos(\phi - \varphi) + H \sin \theta \sin \psi \cos \phi] \\ & - 2K[\sin \psi \sin(\phi - \varphi) \cos \psi_K + \cos \psi \sin \psi_K] \sin \psi \cos(\phi - \varphi) \cos \psi_K \\ & - 4\pi M^2 \sin^2 \psi \sin(\phi - \varphi) \cos(\phi - \varphi) = 0 \end{aligned} \tag{11}$$

is a complicated problem. It can be simplified somewhat if we assume the anisotropy is circular in nature ($\psi_K = 0$).

For the typical parameters of microwire materials ($H_K = 1-5$ Oe; $M \sim 500$ G; cable diameter, 16-38 μm ; measured external fields H of up to 10 Oe; excitation currents i of up to 50 mA; and H_b of up to 6 Oe) that we use in designing and studying sensors, relation $4\pi M \gg H, H_K,$ and $H_b; E_M \gg E_H$ and E_K . The factors that would lead to the emergence of a substantial component of magnetization in radial direction M_r are not found in any region of the wire's surface. The contribution from the demagnetizing field to the energy of the system is thus negligible, and vector \vec{M} can rotate only slightly from the direction of a tangent to the wire surface; i.e., $\phi \approx \varphi \pm 90^\circ$ or $\phi - \varphi \approx \pm 90^\circ, \sin(\phi - \varphi) \approx \pm 1, \sin \phi \approx \pm \cos \varphi, \cos \phi \approx \mp \sin \varphi$.

The choice of the sign before H_K depends on which field (H_b or H_y) determines the slope of vector \vec{M} . When examining the possibilities in terms of equivalent acting fields in the plane of the wire's cross section, there are two ways of orienting the effective field

of anisotropy H_K relative to the direction of the wire's contour. The effect of the anisotropy field coincides with the direction of the action of the predominant factor: the components of all three fields are added for surface points satisfying the condition $-90^\circ < \varphi < 90^\circ$ ($0^\circ < \varphi < 90^\circ$ and $270^\circ < \varphi < 360^\circ$). When actions \vec{H}_y and \vec{H}_b of the field are directed in opposite directions (which occurs at $90^\circ < \varphi < 270^\circ$), H_K is added to the field, the value of which along a given axis is higher in the cylindrical coordinate system,

$$H_{\varphi\Sigma} = H_y \cos \varphi + H_b + H_K \frac{|H_b + H_y \cos \varphi|}{H_b + H_y \cos \varphi}, \tag{12}$$

$$H_{r\Sigma} = H_y \sin \varphi,$$

and in the Cartesian coordinate system,

$$H_{x\Sigma} = -(H_b + H_K) \sin \varphi,$$

$$H_{y\Sigma} = H_y + \left(H_b - H_K \frac{|H_b \cos \varphi + H_y|}{H_b \cos \varphi + H_y} \right) \cos \varphi. \tag{13}$$

The areas of the solution to the problem with respect to the situation on the wire's surface (angle φ) and the sign of the contribution from different factors that determine the orientation of the magnetization vector are shown schematically in Fig. 2. The critical point of the transition from one mode to another is determined by the contributions from \vec{H}_b and \vec{H}_y being equal to zero in the condition of the extremum ($\partial E / \partial \psi = 0$):

$$H_b \sin(\phi - \varphi) + H_y \sin \phi = 0, \tag{14}$$

Where $\sin(\phi - \varphi) \approx 1, \sin \phi \approx \cos \varphi, \cos \phi \approx -\sin \varphi$ for $\phi \approx \varphi + 90^\circ$ and $\sin(\phi - \varphi) \approx -1, \sin \phi \approx -\cos \varphi, \cos \phi \approx \sin \varphi,$ for $\phi \approx \varphi - 90^\circ$. In both cases, $\pm H_b \pm H_y \cos \varphi = 0,$ or $\cos \varphi = -H_b / H_y$. From the resulting system of equations

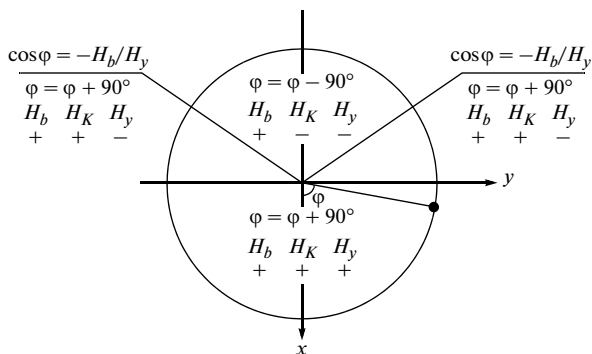


Fig. 2. Classification of the regions of the solution to the problem.

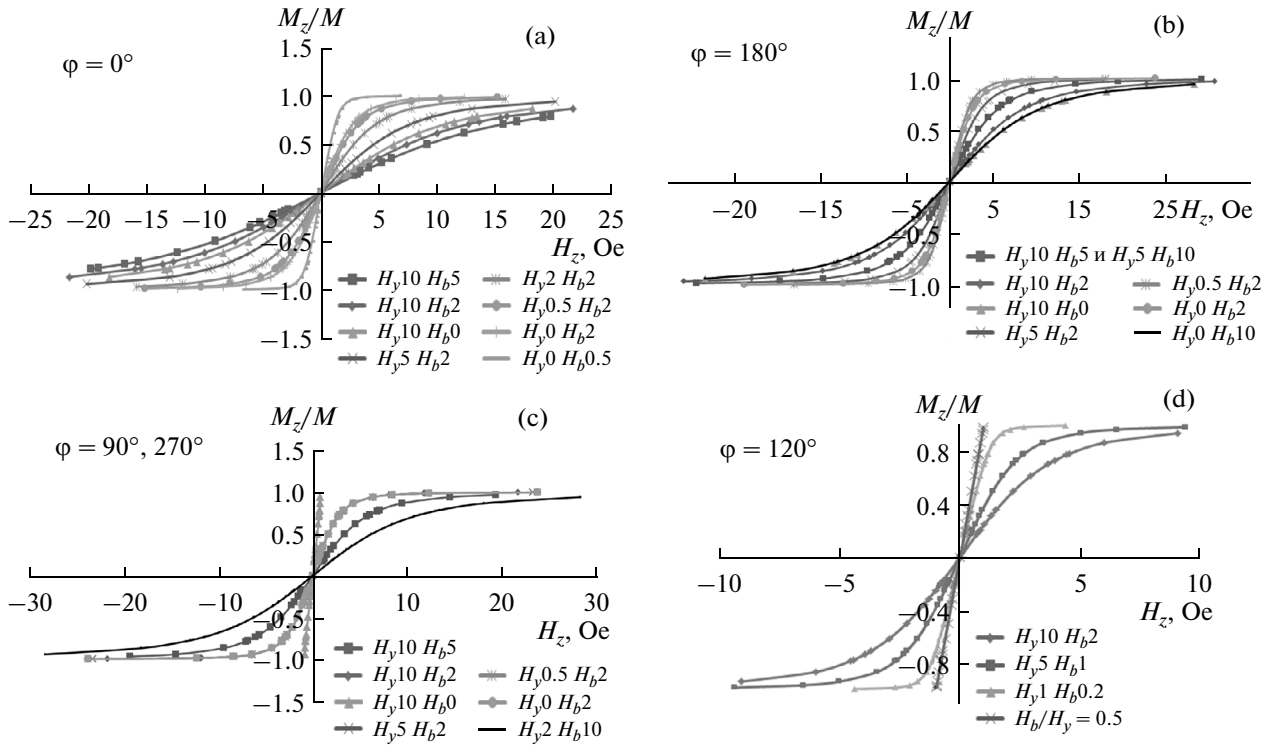


Fig. 3. Relative value of the axial component of magnetization on the surface of a wire with material parameters $H_K = 1$ Oe, $4\pi M = 500$ G at different values of external (H_z and H_y) and circular (H_b) magnetic fields (in oersteds) for characteristic points determined by azimuthal angle φ : (a) 0° , (b) 180° , (c) 90° and 270° , (d) 120° (corresponding to $\arccos(-H_b/H_y)$ at $H_b/H_y = 0.5$).

$$\pm(H_b + H_y \cos \varphi) \cos \psi - H_z \sin \psi + [H_K - (H_K + 4\pi M) \cos^2(\phi - \varphi)] \sin \psi \cos \psi = 0, \quad (15)$$

$$[H_b \pm (H_K + 4\pi M) \sin \psi] \cos(\phi - \varphi) + H_y \cos \phi = 0 \quad (16)$$

we finally obtain the relation for finding angle ψ ,

$$\pm(H_b + H_y \cos \varphi) \cos \psi - H_z \sin \psi \quad (17)$$

$$+ \{H_K - (H_K + 4\pi M)(H_y \sin \varphi)^2 / [H_b \pm (H_K + 4\pi M) \sin \psi]^2\} \sin \psi \cos \psi = 0,$$

which can be simplified by allowing for $4\pi M \gg H_K$,

$$\pm(H_b + H_y \cos \varphi) - H_z \tan \psi + [1 - (4\pi M / H_K)(H_y \sin \varphi)^2 / (H_b \pm 4\pi M \sin \psi)^2] H_K \sin \psi = 0, \quad (18)$$

where the lower sign corresponds to the condition

$$\arccos(-H_b/H_y) < \varphi < 360^\circ - \arccos(-H_b/H_y).$$

At critical point $\varphi_l = -\arccos(-H_b/H_y)$, we have

$$\cos \psi = H_z / \{ [1 - (4\pi M / H_K)(H_y \sin \varphi)^2 / (H_b \pm 4\pi M \sin \psi)^2] H_K \}. \quad (19)$$

In cases of practical importance ($4\pi M \gg H, H_K, H_b$), expression (19) is simplified to

$$M_z/M = \cos \psi = H_z/H_K. \quad (20)$$

Figure 3 shows an example of the distribution of magnetization $M_z/M = \cos \psi$ in the skin layer as a function of the applied magnetic fields following the contour of a wire with parameter $H_K = 1$ Oe, $4\pi M = 500$ G for different positions on its surface φ , obtained by numerically solving Eq. (18). At $\varphi = 0$, transverse component H_y of the external magnetic field increases

the magnetization's angle of deviation from the wire's axis, as does field H_b created by the constant component of the current in the wire (the bias current). At points characterized by azimuths $\varphi = 90^\circ$ and 270° , the angle of the magnetization's deviation does not depend on H_y at the same values of H_b . When $\varphi = 180^\circ$, fields H_y and H_b have an identical effect on ψ but affect the azimuthal orientation of magnetization ϕ in opposite directions. Angle ψ therefore grows or shrinks as transverse field H_y changes, depending on

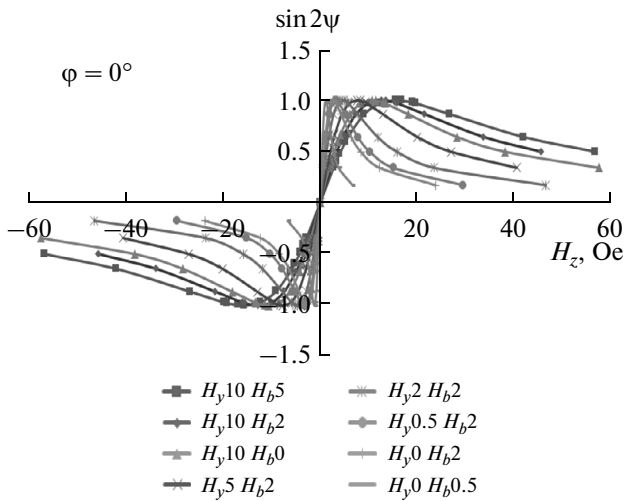


Fig. 4. Plot of the function $\sin 2\psi = f(H_z)$ for the points on the surface of the MI conductor determined by the condition $\varphi = 0$.

the ratio H_b/H_y (when $H_y < H_b$, the transverse field reduces the magnetization's vector of deviation from the axis; a further increase in H_y widens it). At critical points $\varphi = \arccos(-H_b/H_y)$, angle ψ does not depend on the transverse field. As an illustration, Fig. 3d shows the plot for points $\varphi = 120^\circ$ that correspond to the critical value of the azimuthal angle φ_1 at $H_b/H_y = 0.5$. At the ratio $H_b/H_y = 0.2$ $\varphi_1 = 101.5^\circ$, and the orientation of the magnetization vector at these points on the wire's surface depends strongly on the transverse component of the external magnetic field.

Assuming a uniform current density distribution in the skin layer, the signal of the MI element in the inductive configuration of its detection is proportional to the average value of function $\sin 2\psi = f(H_z)$ on the wire's surface, which can be obtained via numerical integration. The plot of this function is shown in Fig. 4 for the points determined by condition $\varphi = 0$. The linear part of the characteristic observed at $H_z < H_K$ is of interest from the viewpoint of using MI in designing sensors, so the descending branch of the plot corresponding to $\psi < 45^\circ$ is not used. The term in the brackets of expression (18) is thus close to unity, and for sensor applications the equation can be written in simplified form:

$$\pm(H_b + H_y \cos \varphi) - H_z \tan \psi + H_K \sin \psi = 0. \quad (21)$$

The effective field representation of magnetic anisotropy gives an adequate picture only near the direction of the easy magnetization, so the influence of the effective field H_K is entirely comparable to the action of real magnetic fields only at orientations of the magnetization near the easy axis of anisotropy. Moving away from this direction, the real influence of magnetic anisotropy is less than the one predicted by

the H_K value, so we must consider the anisotropy constants to perform a strict analysis of the general solution to the problem. Allowing for helicity ($\psi_K \neq 0$) under the above conditions is equivalent to applying additional magnetic biasing along the z -axis of the wire and, by reducing the effect of circular anisotropy, should narrow angle ψ .

CONCLUSIONS

Analysis of the effect magnetic fields of different natures have on the distribution of magnetization in a magnetoimpedance conductor can reveal the conditions under which the transverse component of an external magnetic field does not appreciably affect the signal of the sensor element, opening up the possibility of designing vector (three-dimensional) intellectual magnetic field sensors.

ACKNOWLEDGMENTS

This work was supported by the Russian Foundation for Basic Research, project no. 13-03-01316.

REFERENCES

1. *Magnetic Sensors and Magnetometers*, Ripka, P., Ed., Artech, 2001.
2. Mohri, K., Honkura, Y., Panina, L.V., and Uchiyama, T., *J. Nanosci. Nanotechnol.*, 2012, vol. 12, p. 7491.
3. Yudanov, N.A., Panina, L.V., Morchenko, A.T., Kostishyn, V.G., and Ryapolov, P.A., *J. Nano- Electron. Phys.*, 2013, vol. 5, p. 04004.
4. Makhnovskiy, D.P., Panina, L.V., and Mapps, D.J., *Phys. Rev. B*, 2001, vol. 63, pp. 144424–23.
5. Yudanov N.A., Rudenok A.A., Panina L.V., Morchenko A.T., Kolesnikov A.V., Kostishin V.G., *Bull. Russ. Acad. Sci. Phys.*, 2014, vol. 78, no. 11, p. 1169.
6. Morchenko, A.T. and Panina, L.V., *Fiziko-khimicheskie aspekty izucheniya klasterov, nanostruktur i nanomaterialov: Mezhdunar. sb. nauch. trudov* (Physical and Chemical Aspects for Studying Clusters, Nanostructures and Nanomaterials. Interuniversity Collection of Scientific Works), Tver: Tver State Univ., 2013, issue 5, pp. 180–186.
7. Yudanov, N.A., Rudyonok, A.A., Panina, L.V., Kolesnikov, A.V., Morchenko, A.T., and Kostishyn, V.G., *J. Nano- Electron. Phys.*, 2014, vol. 6, no. 3, p. 03046.
8. Yudanov, N.A., Rudenok, A.A., Kolesnikov, A.V., Panina, L.V., Morchenko, A.T., and Kostishyn, V.G., *Tr. XI Mezhdunar. Konf. "Perspektivnye tekhnologii, oborudovanie i analiticheskie sistemy dlya materialovedeniya i nanomaterialov"* (Proc. 11th Int. Conf. "Promising Technologies, Equipment and Analytical Systems for Material Science and Nanomaterials"), Kursk, May 13–14, 2014, part 2, pp. 388–397.

Translated by L. Mosina